Semiconductor Physics, Quantum Electronics & Optoelectronics, 2020. V. 23, No 2. P. 193-200.

Optics

Light-emitting properties of BN synthesized by different techniques

G.Yu. Rudko[1,2], L.L. Sartinska[3], O.F. Isaieva[1,2], E.G. Gule[1], T. Eren[4], E. Altay[4]

[1]*Institute of Physics, NAS of Ukraine,*
41, prospect Nauky, 03680 Kyiv, Ukraine
[2]*National University "Kyiv-Mohyla Academy",*
2, Skovorody str., 04070 Kyiv, Ukraine
[3]*I. Frantsevich Institute for Problems of Materials Science, NAS of Ukraine,*
3, Krzhyzhanovsky str., 03680 Kyiv-142, Ukraine
[4]*Yildiz Technical University, Chemistry Department,*
Davutpasa Campus, 34220 Esenler, Istanbul, Turkey
[*]*E-mail: g.yu.rudko@gmail.com*

Abstract. Light-emitting properties of boron nitride powders of different morphology grown using various techniques have been studied. All samples were hexagonal BN (h-BN), while the content of impurity phases varied considerably. The wide photoluminescence band in the visible range has been observed. h-BN synthesized using carbothermal reduction method exhibited the highest efficiency of the photoluminescence emission. The intensity of BN emission has been interpreted in terms of interplay between the emission of intrinsic defects stabilized by carbon, carbon-related recombination centers and the centers of non-radiative recombination caused by the presence of sassolite phases in the samples.

Keywords: boron nitride, nanostructures, XRD, SEM, photoluminescence.

https://doi.org/10.15407/spqeo23.02.193
PACS 78.55.-m, 78.55 Hx, 78.67.-n

Manuscript received 06.02.20; revised version received 27.03.20; accepted for publication 10.06.20; published online 12.06.20.

1. Introduction

Search for advanced materials with enhanced properties for optoelectronic devices of new generation stimulates investigations of semiconductors with wide band gap including group III nitrides. One of the most interesting representatives of this class is the synthetic chemical compound boron nitride (BN). Since it is well-known that lowering the dimensionality is an effective way to broaden the application fields of materials, special attention is also paid to nanostructured boron nitride materials. Nano-BN has the bandgap energy close to 6 eV and forms large diversity of structures, including those conformable to graphine, carbon nanotubes, nanofibers, *etc*. Nanostructured BN displays various attractive electronic, optical and magnetic properties (for the review, see [1]) that are advantageous for applications in electronic devices, high heat-resistant semiconductors and insulator lubricants [2–6]. At present, the BN-based devices for hydrogen storage [2–4], composites, where nano-BN is used as a filler [5], and abrasive materials [6] have been demonstrated.

One more aspect of the increasing attention to nano-BN is related with its light-emitting properties [7–22]. It is known that bulk hexagonal boron nitride, being excited either by accelerated electrons beam or by far UV radiation, is a good light emitter in deep ultraviolet [7–9]. *E.g*., it was shown in [7] that h-BN can emit intense 215-nanometer luminescence at room temperature, and this emission was ascribed to free exciton luminescence. Moreover, in [9] the lasing effect at this wavelength was observed in hexagonal boron nitride single crystals. In view of increasing requirements to compact ultraviolet laser devices, these phenomena make h-BN a promising material for applications in optical storage, photo-catalysis, and nanosurgery.

Bulk h-BN is also fluorescent in the visible range under optical excitation above 4 eV [10–12], which makes h-BN material suitable for creation of display and lighting devices. Visible luminescence of bulk BN forms a wide phonon-assisted emission band with asymmetric profile: it peaks in the violet-blue region and has a long tail to the low energy side ranging to green-orange region [13–15]. Visible luminescence can be excited either via band-to-band excitation or via defect-related intraband states [13, 14].

Similarly to bulk BN, nano-BN also emits light both in the UV and visible ranges [14, 16-18]. Moreover, nano-BN with a high content of oxygen and carbon, often named BCNO [19–22], is also an efficient luminophore. Therefore, BN-based nano-materials are expected to be used in nanosize light sources, light emitting display devices, and medical diagnostic devices. Combination of good mechanical properties, thermo- and wear-resistance

with the emission of light paves the way to fabrication of nano-luminophores with advanced properties, which could meet the strict requirements for operation in severe environmental conditions. Thus, the aim of this work is to study light-emitting properties of the powders of nanostructured BN possessing different morphology and produced using various growth methods.

2. Experimental

Four types of nano-BN powders were studied (Table). Nano-BN samples of the type A were synthesized using the reaction of carbothermal reduction [23]. The samples of types B and C were produced from chemically pure boron by using the high-temperature catalyst-free synthesis [25, 26] in an optical furnace in the flow of nitrogen. The grain sizes of initial boron powder were 0.05 μm and 2.00 μm for the samples B and C, respectively. Detailed description of these initial powders and their electron microscopy images were presented in [27]. As a result of catalyst-free synthesis, the black color of boron precursor turned into the white one. The presence of moisture in the flow of nitrogen can lead to formation of oxygen-containing components in the BN powder material. Commercially available BN powder produced by Chempur Company was used as reference sample for comparison (type D samples). The structure of BN nano-powders was examined using scanning electron microscopy (SEM) with JEOL Superprobe 733 electron microprobe. Crystallinity and phase composition of the powders were characterized by XRD diffractometer "DRON-3.0" (CuK_α radiation).

Optical properties of nano-BN were characterized using the photoluminescence (PL) method. The light sources LED-DUV-280-OC46 (280 nm, 2.6 mW) and LED-NS375L-5RLO (375 nm, 6 mW) were used for excitation of light emission. The emitted light was dispersed by MDR-12 monochromator and detected with a lock-in photomultiplier-based scheme. The filters were inserted in front of the monochromator slit to cut off the excitation light (the filters BS-4 for λ_{exc} = 280 nm and GS-10 for λ_{exc} = 375 nm). All the measurements were performed at room temperature.

3. Results

SEM images of A, B, C and D samples and corresponding histograms of particle size distributions are shown in Fig. 1 (a–d) and Fig. 2 (a–d), respectively. The sample A synthesized in the process of carbothermal reduction is an agglomerate of partially molten particles (Fig. 1a). Their size distribution is rather wide (Fig. 2a); the weighted average size of the particles is about 600 nm. The sample B produced in the optical furnace from the boron powder (mean size of grains is close to 0.05 μm) is composed of fine-grained and clearly visible flake-like BN particles, which have sizes of about 300 nm and thickness almost by an order of magnitude smaller; these flakes form agglomerates with the sizes 1…2 μm (Figs 1b and 2b). Nanoparticles of the sample C formed in the optical furnace from boron powder (2.00 μm) are flake-like (Fig. 1c). The mean size of these particles is about 400 nm (Fig. 2c). The thickness of flakes in C samples is similar to that of the samples B particles (Figs 1b and 1c). The dispersion of flake size distribution for the sample C is rather wide (Fig. 2c). Note that nano-flakes in the sample C do not show a tendency to agglomerate. The sample D (commercially available BN) consists of nano-flakes with the mean size close to 550 nm, which form agglomerates with a size of several micrometers (Figs 1d and 2d).

Table. Samples characteristics.

Sample type	Precursors	Method of BN synthesis	Reaction conditions for synthesis
A	Boron oxide Saccharose Nitrogen gas	Carbothermal reduction	Annealing in the furnace under nitrogen atmosphere (T = 1000…1450 °C)
B	Boron powder (0.05 μm) Flow of nitrogen	Direct synthesis in a high-power optical furnace	Heating under concentrated light (T = 1400…1700 °C)
C	Boron powder (2.00 μm) Flow of nitrogen	Direct synthesis in a high-power optical furnace	Heating under concentrated light (T = 1400…1700 °C)
D	Commercially available BN (Chempur company), growth details are not available		

Crystallinity and phase composition of these BN powders was characterized using XRD measurements (Fig. 3). XRD patterns of all the samples demonstrate (002), (100), (101) and (004) diffraction peaks that correspond to the hexagonal phase of BN (the arrow under each graph indicates the position of corresponding peak) [3, 27, 28]. Beside the reflections of crystalline h-BN, XRD diffractograms of all the samples reveal the presence of some oxygen- and/or hydrogen-containing phases. The most pure material is the commercial one (sample D). It contains only a small amount of boron oxide B_2O_3 impurity. However, the average size of particles in commercial samples is the largest. Note that the diffractograms of all other samples do not reveal the presence of B_2O_3 phase. The samples B and C contain large amounts of sassolite (boric acid H_3BO_3). Boric acid is the product of reaction between boron and moisture; the latter is present in the nitrogen flow used for synthesizing the samples. Sassolite can also be seen in the XRD diffractogram of the sample A grown by carbothermal reduction of boron oxide, however, the fraction of sassolite in the sample A is obviously smaller than in B and C samples. Note that the sample A, most probably, contains unreacted carbon, because it is well-known that carbothermal reduction method provides the material strongly contaminated with unreacted charcoal (see, *e.g.*, [24]). However, identification of carbon clusters by their diffraction pattern is not possible in this material, since the most intense peak of carbon particles ([002] – 26.5°) overlaps with the [002] peak of BN (26.27°) [29–31].

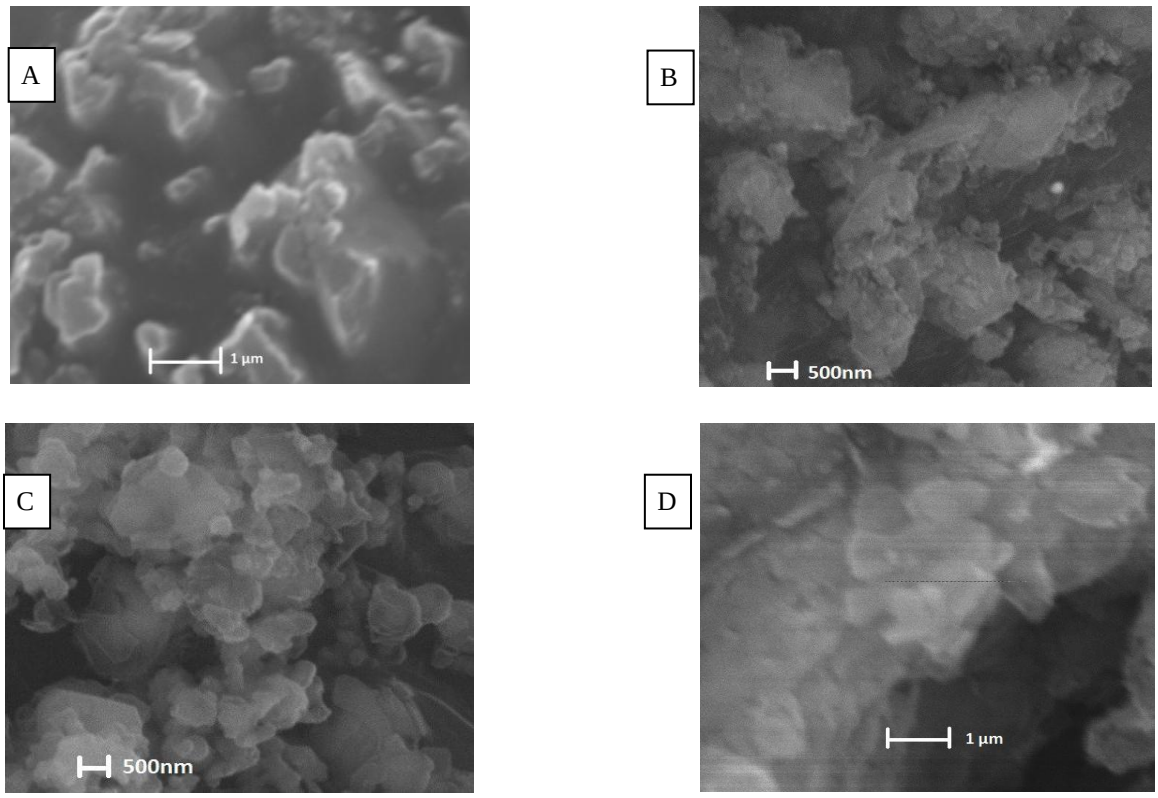

Fig. 1. SEM images of BN samples prepared using various methods: A – carbothermal reduction; B and C – direct synthesis in a high-power optical furnace from the boron powders with the grain sizes of 0.05 and 2.00 μm, respectively; D – commercially available BN powder (Chempur Company).

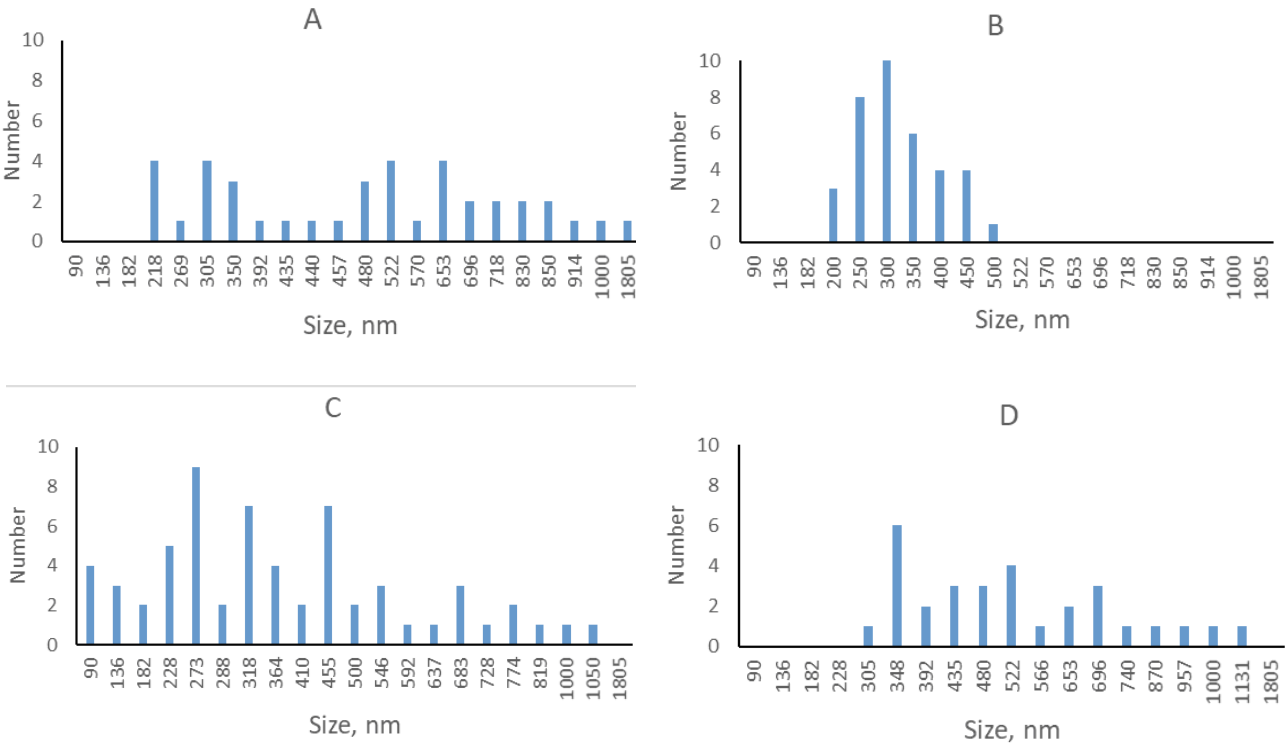

Fig. 2. Size distribution of BN particles based on SEM images.

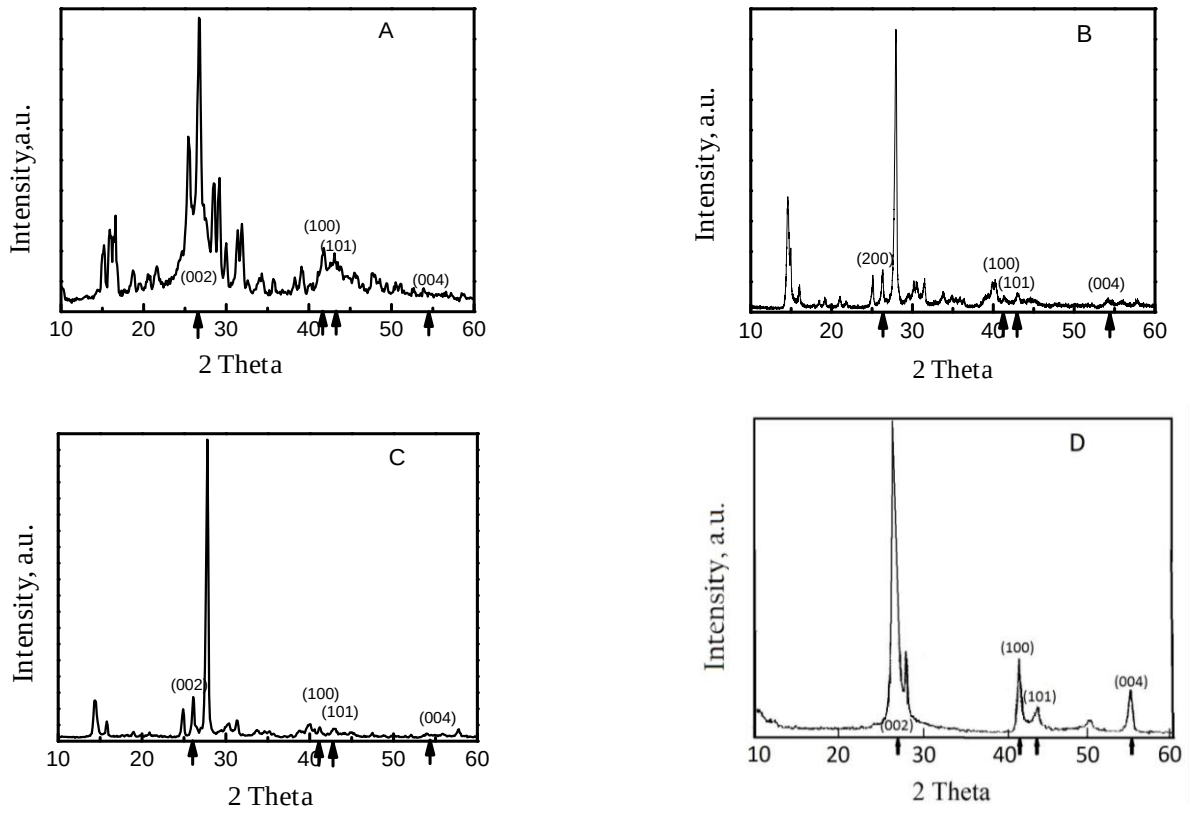

Fig. 3. XRD diffractograms of the samples A, B, C, D.

Results of the photoluminescence studies of nano-BN samples obtained by different synthesis procedures are shown in Fig. 4a (excitation with λ_{exc} = 280 nm) and in Fig. 4b (excitation with λ_{exc} = 375 nm). The energies of the exciting light quanta in both cases (~4.4 eV and ~3.3 eV, respectively) are not sufficient for band-to-band excitation. Indeed, according to the literature data [2, 10, 11, 16, 32, 33] the band gap of h-BN varies from ~5 eV [2, 32] to ~6 eV [33] depending on the synthesis method, morphology, impurity composition, *etc*. Nevertheless, the sub-gap excitation of BN is quite usual [16, 17, 19, 21, 34–39]. Previously, it has been shown that it is possible to excite the emission of pure and doped nano-BN with the quanta smaller than E_g. For example, to achieve excitation of BN luminescence via defect-related levels inside the band gap, the authors of [16, 17, 21, 34, 35] used the light with the quanta energy about ~4.4 eV, and the authors of [19, 21, 38, 39] used quanta with the energy close to 3.3 eV.

From Fig. 4a, it is seen that under excitation with λ_{exc} = 280 nm the h-BN samples A, C and D demonstrate rather wide luminescence band in the visible spectral range with slightly different maxima positions varying from 400 up to 425 nm (3.1…2.9 eV). Fig. 4a shows that the efficiency of light emission strongly depends on the procedure of h-BN powders formation. The highest intensity of emission is observed for A sample. Its integrated emission intensity is about 2.5 times higher than that of the sample D, when these two samples are measured side by side for a direct comparison. Unfortunately, precise comparison of the emission efficiencies is impossible, since all the initial samples are powder-like. Therefore, for optical studies we prepared homogeneous layers of powder by distributing initial BN powders over the surface of sticky conducting scotch (this scotch is non-light-emitting by itself). Thus, the density of the light-emitting layer of BN powder can vary by several percents, which, correspondingly, causes deviations in the intensity of photoluminescence signals. Note that the emission of the samples A and D can be seen by the naked eye and is perceived as bluish white. It is illustrated by the photo in the insert in Fig. 4a. Here, the white light-emitting spot in the center is the place where the exciting beam hits the surface of the sample A. It is this emission that is analyzed by the monochromator and corresponds to the curve *A* in Fig. 4a. The blue halo around the white spot corresponds to the light that was multiply scattered, re-absorbed and re-emitted in the h-BN powder around the excitation spot. From Fig. 4a, it is also seen that the sample B grown using catalyst-free synthesis in optical furnace is much less efficient as a light-emitting material, while luminescence of the sample C is almost negligible.

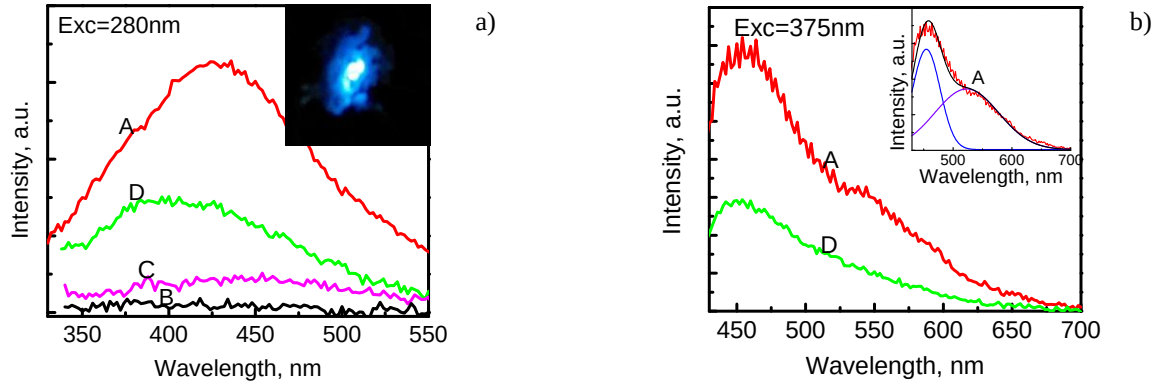

Fig. 4. Photoluminescence spectra of the nano-BN samples A, B, C, D obtained using different synthesis procedures: a) excitation wavelength 280 nm, b) excitation wavelength 375 nm. Insert in Fig. 4a – the photo of emission (sample A). Insert in Fig. 4b – fitting of the curve A with two Gaussians.

Fig. 4b shows PL spectra of the samples A and D measured at the excitation λ_{exc} = 375 nm; no signals from the samples B and C were observed at this excitation.

Note that short-wave parts of the spectra cannot be registered at the latter excitation, because the exciting light hits the left wing of the PL band. It can be seen that excitation with λ_{exc} = 375 nm reveals an additional feature in the long-wave part of the sample A spectrum; the latter corresponds to the emission of some additional light-emitting defect centers that do not exist in other samples and emit in the orange-red spectral range. On the contrary, the spectrum of the sample D remains unchanged.

4. Discussion

The samples of h-BN under study differ very much in their morphology, average sizes of particles and purity. XRD measurements showed that all the samples contain hexagonal BN, while the content of impurity phases varies considerably depending on the synthesis route. A, B, C samples contain large amounts of sassolite, while D does not. The latter contains only small amount of B_2O_3. In what follows, we will discuss the role of these additional phases in the light emission by BN powders.

Despite the described diversity of morphology and composition, all the samples, excepting the sample B, demonstrate similar broad structureless emission band in the visible range at the excitation with λ_{exc} = 280 nm (4.4 eV). The intensity of this band strongly varies with the synthesis method, while the position of the maximum remains almost the same. The spectral position of this band (near 3 eV) evidences that this emission occurs via energy levels within the band gap, which can originate either from intrinsic defects or impurities. The luminescence band observed in our samples is similar to those reported for bulk BN and nano-BN in [16, 17, 19, 32, 40] as well as for BCN and BCNO in [19, 21, 38, 41]. Usually, this emission is interpreted as that dependent on the available impurities and sample preparation conditions (see, *e.g.* [10, 32, 39, 41]).

The observed differences in the efficiencies of light emission can be caused either by different concentrations of light-emitting centers or luminescence quenching centers in the samples. Among the models of light-emitting centers, the so-called "one-boron" and "three-boron" centers [10, 32] seem to be well argumented by EPR studies. The three-boron centers are electrons trapped in nitrogen vacancies, one-boron centers are supposed to be related to boron oxide. Therefore, three-boron centers are a plausible source of luminescence in all the samples, while the one-boron ones, most probably, are characteristic for the sample D. It should be noted that in the papers [10, 32] it was stressed that three-boron centers appear only in the presence of carbon. Moreover, the admixture of carbon and oxygen to BN has been proven to be advantageous for observation of visible light emission [19, 21, 38]. In view of these findings, the highest efficiency of luminescence in the sample A prepared using carbothermal reduction of boron oxide can be ascribed to the highest content of carbon in this sample. One more confirmation of the role of carbon can be found in the insert in Fig. 4b. It shows the fitting of the emission spectrum of the sample A obtained under λ_{exc} = 375 nm. Two Gaussians were used for this fitting. It is seen that the additional feature that emerges in the long-wave side of the spectrum can be pretty well described by the band with the maximum at ~550 nm. Similar bands were observed in BCNO [19, 21] and even for carbon clusters incorporated into solid SiO_2 matrix [42, 43], thus the band at ~550 nm can be ascribed to carbon-related species in BN.

As it was mentioned above, the integral emission intensity is also governed (besides the number of emitting centers) by the rate of non-radiative transitions. The centers of non-radiative recombination can provide the paths for excited electron-hole pairs to recombine without emitting light quanta. In view of the increasing role of surface-related quenching in nanoparticles, the non-radiative deterioration of light emission in nano-BN is quite plausible. It is especially true for the sample B that has the particles of the smallest sizes. However,

this does not hold for the sample C that also has poor light emitting properties, but the BN particles are comparable with the samples A and D. Therefore, it is reasonable to suppose that the samples B and C contain the centers of non-radiative emission that are not related to the surface. The most plausible candidate for the luminescence quencher is the presence of the additional phase of sassolite, because the content of sassolite dominates in the samples with the lowest luminescence efficiency.

5. Conclusions

Four types of nano-BN samples have been studied by SEM, XRD and photoluminescence methods. Two samples were synthesized using boron as a precursor, one sample – using boron oxide as a precursor, and one commercial sample was used for comparison. All the samples differ very much in their morphology, average sizes of particles (from 300 up to 600 nm) and purity. The samples demonstrate very wide luminescence bands in the visible range with the maxima positions varying from 400 up to 425 nm (λ_{exc} = 280 nm), *i.e*., the radiative recombination occurs via the energy levels of deep defects. As compared with the samples synthesized using carbothermal reduction of boron oxide and commercial BN, the intensity of nano-BN samples grown in the optical furnace is much lower. Excitation with the light λ_{exc} = 375 nm reveals additional band in BN grown in the process of carbothermal reduction of boron oxide as compared with the commercial BN and BN grown in the optical furnace. This feature is ascribed to the presence of carbon impurity in the sample.

Intensity of the emission related to BN is interpreted in terms of interplay between the emission of intrinsic defects stabilized by carbon, carbon-related recombination centers and the centers of non-radiative recombination caused by the presence of sassolite phases in the samples.

Acknowledgement

The authors (G. Rudko, O. Isaieva, E. Gule) acknowledge financial support from NAS of Ukraine, grant # 0116U002611.

References

1. Chkhartishvili L. Boron nitride nanostructures: Molecules, sheets, tubes, fullerenes (An overview). *Nano Stud.* 2010. **2** (March). P. 139–174. https://doi.org/10.1088/1742-6596/176/1/012014.
2. Weng Q., Wang X., Zhi Ch., Bando Y., Golberg D. Boron nitride porous microbelts for hydrogen storage. *ACS Nano*. 2013. **7**, No 2. P. 1558–1565. https://doi.org/10.1021/nn305320v.
3. Moussa G., Salameh Ch., Bruma A. *et al.* Nanostructured boron nitride: From molecular design to hydrogen storage application. *Inorganics*. 2014. **2**, No 3. P. 396–409. https://doi.org/10.3390/inorganics2030396.
4. Cheng Y., Zhang Ch., Ren J., Tong K. Hydrogen storage in Li-doped fullerene-intercalated hexagonal boron nitrogen layer. *Frontiers of Physics.* 2016. **11**, No 5. P. 13101. https://doi.org/10.1007/s11467-016-0559-4.
5. Pakdel A., Bando Y. and Golberg D. Nano boron nitride flatland. *Chem. Soc. Rev*. 2014. **43**. P. 934–959. https://doi.org/10.1039/c3cs60260e.
6. Reich S., Ferrari A.C., Arenal R., Loiseau A., Bello I. Resonant Raman scattering in cubic and hexagonal boron nitride. *Phys. Rev. B*. 2005. **71**. P. 205201-1. https://doi.org/10.1103/PhysRevB.71.205201.
7. Kubota Y., Watanabe K., Tsuda O., and Taniguchi T. Deep ultraviolet light-emitting hexagonal boron nitride synthesized at atmospheric pressure. *Science*. 2007. **317**(5840). P. 932–934. https://doi.org/10.1126/science.1144216.
8. Watanabe K., Taniguchi T., Kuroda T., and Kanda H. Band-edge luminescence of deformed hexagonal boron nitride single crystals. *Diamond and Related Materials*. 2006. **15**, No 11-12. P. 1891–1893. https://doi.org/10.1016/j.diamond.2006.06.014.
9. Watanabe K., Taniguchi T., Kanda H. Direct-bandgap properties and evidence for ultraviolet lasing of hexagonal boron nitride single crystal. *Nature Mater.* 2004. **3**. P. 404–409. https://doi.org/10.1038/nmat1134.
10. Katzir A., Suss J.T., Zunger A., Halperin A. Point defects in hexagonal boron nitride. I. EPR, thermoluminescence, and thermally-stimulated-current measurements. *Phys. Rev. B*. 1975. **11**. P. 2370. https://doi.org/10.1103/PhysRevB.11.2370.
11. Solozhenko V., Lazarenko A., Petitet J., Kanaev A. Bandgap energy of graphite-like hexagonal boron nitride. *J. Phys. Chem. Solids*. 2001. **62**, No 7. P. 1331-1334. https://doi.org/10.1016/S0022-3697(01)00030-0.
12. Kanaeva A., Petitet J. Femtosecond and ultraviolet laser irradiation of graphite-like hexagonal boron nitride. *J. Appl. Phys*. 2004. **96**. P. 4483. https://doi.org/10.1063/1.1787909.
13. Berzina B., Korsaks V., Trinkler L., Sarakovskis A., Grube J., and Bellucci S. Defect-induced blue luminescence of hexagonal boron nitride. *Diamond and Related Materials*. 2016. **68**. P. 131–137. https://doi.org/10.1016/j.diamond.2016.06.010.
14. Korsaks V., Berzina B., Trinklere L. Low-temperature 450 nm luminescence of hexagonal boron nitride. *Latvian J. Phys. Techn. Sci.* 2011. **48**, No 1. P. 55–60. https://doi.org/10.2478/v10047-011-0005-x.
15. Museur L., Kanaev A. Photoluminescence properties of pyrolytic boron nitride. *J. Mater. Sci.* 2009. **44**, No 10. P. 2560–2565. https://doi.org/10.1007/s10853-009-3334-x.
16. Berzina B., Trinkler L., Korsak V. *et al.* Exciton luminescence of boron nitride nanotubes and nano-arches. *phys. status solidi* (*b*). 2006. **243**, No 14. P. 3840–3845. https://doi.org/10.1002/pssb.200672108.
17. Chen H., Chen Y., Liu Y., Xu C., Williams J. Light emission and excitonic effect of boron nitride nanotubes observed by photoluminescent spectra.

Opt. Mater. 2007. **29**, No 11. P. 1295–1298. https://doi.org/10.1016/j.optmat.2006.05.006.
18. Chen Zh., Zou J., Liu G. *et al.* Novel boron nitride hollow nanoribbons. *ACS Nano*. 2008. **2**, No 10. P. 2183–2191. https://doi.org/10.1021/nn8004922.
19. Xue Q., Zhang H., Zhu M. *et al.* Hydrothermal synthesis of blue-fluorescent monolayer BN and BCNO quantum dots for bio-imaging probes. *RSC Adv.* 2016. **6**. P. 79090–79094. https://doi.org/10.1039/C6RA16744F.
20. Zhang X., Lu Z., Lin J. *et al.* Luminescence properties of BCNO phosphor prepared by a green and simple method. *Mater. Lett.* 2013. **94**. P. 72–75. https://doi.org/10.1016/j.matlet.2012.12.020.
21. Zhang X., Li L., Lu Z. *et al.* Effects of carbon and oxygen impurities on luminescence properties of BCNO phosphor. *J. Amer. Ceram. Soc.* 2014. **97**, No 1. P. 246–250. https://doi.org/10.1111/jace.12645.
22. Zhang X., Jia X., Liu H. *et al.* Spectral properties and luminescence mechanism of red emitting BCNO phosphors. *RSC Adv*. 2015. **5**. P. 40864–40871. https://doi.org/10.1039/C5RA07054F.
23. Bartnitskaya T.S., Vlasova M.V., Kosolapova T.Ya. *et al*. Formation of boron nitride during carbothermal reduction. *Soviet Powder Metallurgy and Metal Ceramics*. 1990. **29**, No 12. P. 990–994. https://doi.org/10.1007/BF00793385.
24. Aydoğdu A., Sevinç N. Carbothermic formation of boron nitride. *J. Eur. Ceram. Soc*. 2003. **23**, No 16. P. 3153–3161. https://doi.org/10.1016/S0955-2219(03)00092-X.
25. Sartinska L., Frolov A., Koval Y. *et al*. Transformation of fine-grained graphite-like boron nitride induced by concentrated light energy. *Mater. Chem. Phys.* 2008. **109**, No 1. P. 20–25. https://doi.org/10.1016/j.matchemphys.2007.10.043.
26. Frolov A., Sartinska L., Koval' Y., Danilenko N. Application of the optical furnace for nanosized boron nitride production. *Nanomater*. 2008. **2**, No. 4 P. 115–120 (in Russian).
27. Sartinska L., Eren T., Altay E., Frolov G. Effect of moisture on the boron nitride formation from elements in a xenon high flux optical furnace. *Eur. Chem. Bull*. 2015. **4**, No 3. P. 165–168.
28. Li J., Lin H., Chen Y., Su Q., Bi X. Synthesis and anti-oxidation performance of nanoflake-decorated boron nitride hollow microspheres. *J. Alloys Compounds*. 2013. **550**. P. 292–296. https://doi.org/10.1016/j.jallcom.2012.09.084.
29. Kakiage M., Shoji T., Kobayashi H. Low-temperature carbothermal nitridation of boron oxide induced by networked carbon structure. *J. Ceram. Soc. Jpn*. 2016. **124**, No 1. P. 13–17. https://doi.org/10.2109/jcersj2.15197.
30. Miao X., Qu D., Yang D. *et al.* Synthesis of carbon dots with multiple color emission by controlled graphitization and surface functionalization. *Adv. Mater*. 2018. **30**, No 1. P. 1704740. https://doi.org/10.1002/adma.201704740.
31. Huang C., Chen C., Ye X. *et al.* Stable colloidal boron nitride nanosheet dispersion and its potential application in catalysis. *J. Mater. Chem. A*. 2013. **1**. P. 12192–12197. https://doi.org/10.1039/C3TA12231J.
32. Lopatin V., Konusov F. Energetic states in the boron nitride band gap. *J. Phys. Chem. Solids.* 1992. **53**, No 6. P. 847–854. https://doi.org/10.1016/0022-3697(92)90199-N.
33. Cassabois G., Valvin P., Gil B. Hexagonal boron nitride is an indirect bandgap semiconductor. *Nature Photon*. 2016. **10**. P. 262–266. https://doi.org/10.1038/nphoton.2015.277.
34. Williams R., Ucer K., Carroll D. *et al.* Photoluminescence of self-trapped excitons in boron nitride nanotubes. *J. Nanosci. Nanotechnol*. 2008. **8**, No 12. P. 6504–6508. https://doi.org/10.1166/jnn.2008.005.
35. Wu J., Han W., Walukiewicz W. *et al.* Raman spectroscopy and time-resolved photoluminescence of BN and $B_xC_yN_z$ nanotubes. *Nano Lett*. 2004. **4**, No 4. P. 647–650. https://doi.org/10.1021/nl049862e.
36. Silly M., Jaffrennou P., Barjon J. *et al.* Luminescence properties of hexagonal boron nitride: Cathodoluminescence and photoluminescence spectroscopy measurements. *Phys. Rev. B*. 2007. **75**. P. 085205. https://doi.org/10.1103/PhysRevB.75.085205.
37. Vokhmintsev A., Weinstein I., Zamyatin D. Electron-phonon interactions in subband excited photoluminescence of hexagonal boron nitride. *J. Lumin*. 2019. **208**. P. 363–370. https://doi.org/10.1016/j.jlumin.2018.12.036.
38. Bhattacharyya P., Sahoo S., Seikh A. *et al.* Synthesis, characterization and optical property study of BCNO and BCN related nanopowder. *Diamond and Related Materials*. 2019. **92**. P. 235–241. https://doi.org/10.1016/j.diamond.2019.01.006.
39. Wang J., Ma F., Liang W., Wang R., Sun M. Optical, photonic and optoelectronic properties of graphene, h-NB and their hybrid materials. *Nanophotonics*. 2017. **6**, No 5. P. 943–976. https://doi.org/10.1515/nanoph-2017-0015.
40. Berzina B., Trinkler L., Krutohvostov R. *et al.* Photoluminescence excitation spectroscopy in boron nitride nanotubes compared to micro-crystalline h-BN and c-BN. *phys. status solidi* (*c*). 2005. **2**, No 1. P. 318–321. https://doi.org/10.1002/pssc.200460174.
41. Chu Z., Kang Y., Jiang Z. *et al.* Graphene oxide based BCNO hybrid nanostructures: tunable band gaps for full colour white emission. *RSC Adv*. 2014. **4**. P. 26855–26860. https://doi.org/10.1039/C4RA02775B.
42. Vasin A., Rusavsky A., Nazarov A. *et al*. Excitation effects and luminescence stability in porous SiO_2:C layers. *phys. status solidi* (*a*). 2012. **209**. P. 1015–1021. https://doi.org/10.1002/pssa.201100815.
43. Vasin A., Verovsky I., Tyortykh V. *et al*. The effect of incorporation of hydrocarbon groups on visible photoluminescence of thermally treated fumed silica. *J. Nano Res.* 2016. **39**. P. 80–88. https://doi.org/10.4028/www.scientific.net/JNanoR.39.80.

Authors and CV

Galina Yu. Rudko, Leading Researcher at the V. Lashkaryov Institute of Semiconductor Physics, NAS of Ukraine, Professor, Doctor of Sciences. The area of scientific interests includes optical and structural properties of semiconductors, related nanostructures and composite materials.

Lina L. Sartinska, Senior Researcher at the Institute for Problems of Materials Sciences, NAS of Ukraine. Candidate of Technical Sciences (Powder Metallurgy and Composite Materials). The area of her scientific interests is materials science with the focus on the technology of superhard materials.

Oksana F. Isaieva, Ph.D student at the V. Lashkaryov Institute of Semiconductor Physics, NAS of Ukraine. The area of scientific interests is optics of nanomaterials.

Evgen G. Gule, Scientific Researcher at the V. Lashkaryov Institute of Semiconductor Physics, NAS of Ukraine. The area of scientific interests includes optical properties of semiconductors and nanostructures.

Tarik Eren, Professor, Doctor of Sciences at the Yildiz Technical University, Turkey. The area of scientific interests includes physical chemistry, materials chemistry, functional materials.

Esra Altay, Ph.D at the Yildiz Technical University, Turkey. The area of scientific interests includes materials chemistry, surface chemistry, materials engineering.